Electronic Supplementary Material (ESI) for Journal of Materials Chemistry C.

Supporting Information

Amino-Acid-Directed Formation of Quasi-Zero-Dimensional Perovskites for High-Purity Blue and Red Luminescence

Baisheng Zhu,[1] Tian Wang,[1] Zhi-Kuang Tan[1,2]*

[1]*Department of Chemistry, National University of Singapore, 3 Science Drive 3, 117543, Singapore*

[2]*Solar Energy Research Institute of Singapore, National University of Singapore, 7 Engineering Drive 1, 117574, Singapore*

* Correspondence to chmtanz@nus.edu.sg

Density functional theory calculations

All density functional theory (DFT) calculations were performed using the Vienna *Ab initio* Simulation Package (VASP).[1] The electron-ion interaction was described by the projector augmented wave (PAW)[2] method with an energy cutoff of 400 eV for the plane-wave basis set. As for the exchange-correlation functional, the generalized gradient approximation (GGA) of Perdew-Burke-Ernzerhof (PBE) is used.[3] A Gamma centered 3 × 3 × 1 Monkhorst-Pack mesh was adapted for sampling the Brillouin zone of the perovskite (001) slabs. The perovskite slab is constructed on its (001) direction with 7 atomic layers on its z-direction and a 2 × 2 supercell on its x- and y-directions. The (001) surfaces are terminated by the CsBr layer. A 20 Å vacuum is adapted to the slab model. The atomic positions were optimized according to the atomic forces with a threshold that the force on each atom was less than 0.02 eV/Å. The dispersion correction of Grimme's dispersion method with Becke-Johnson damping (GD3-BJ) were included during the structural optimization.[4] The adsorption energy (E_{ads}) is calculated as:

$$E_{\text{ads}} = E(\text{slab+ligand}) - E(\text{slab}) - E(\text{ligand})$$

where E(slab+ligand) is the total energy of slab with 3-APA ligand attached, E(slab) is the energy of the perovskite slab, and E(ligand) is the energy of the isolated 3-APA ligand inside a 30 × 31 × 32 $Å^3$ lattice. As E(slab+ligand) involves the calculation of a charged slab, the total energy E(slab+ligand) of the charged slab is further corrected by the self-consistent potential correction method (SCPC).[5] The total energy can be written as:

$$E(\text{slab+ligand}) = E(\text{SCPC}) + qV_{\text{alig}}$$

where E(SCPC) is the SCPC total energy using neutral system as reference, q is the total charge (+1) of our system, and V_{alig} is the potential alignment. The vacuum slab is increased to 65 Å (3 times of the perovskite slab thickness) for SCPC method. The interface is set at 1.5 Å away from the edge of the perovskite slab. The relative macroscopic dielectric constant is set to be 2.09 to represent the 1-octadecene (refractive index of 1.445) environment.

Table S1. The corresponding PL decay parameters of perovskite films are listed below.

Sample	PLQY/%	τ/ns	$K_r/\mu s^{-1}$	$K_{nr}/\mu s^{-1}$	K_r/K_{nr}/%
CsBr-1.0	38.6	9.1	42.4	67.5	62.8
CsBr-1.1	36.3	8.5	42.7	75.0	56.9
CsBr-1.2	40.1	9.3	43.1	64.1	67.2
CsBr-1.3	27.4	7.6	36.0	95.5	37.7
CsBr-1.4	20.8	7.5	27.7	105.6	26.2
CsBr-1.5	14.1	7.3	19.3	117.7	16.4
CsBr-1.6	5.4	7.2	7.5	131.4	5.7

(K_r stands for radiative recombination rate, K_{nr} stands for nonradiative recombination rate, τ stands for an average lifetime.)

Time-resolved PL decays are acquired using a time-correlated single photon counting (TCSPC) setup. The PL decay curves are fitted using an exponential equation: $I(t) = A\exp(-t/\tau)$, where A is the amplitudes of the exponential terms while τ is the PL lifetime. I stands for the normalized PL intensity and t is the time. The PLQY is defined as the ratio of the radiative recombination rate constant (K_r) to the sum of the radiative and non-radiative recombination rate constant (K_{nr}), given by equation

$$PLQY = K_r/(K_r+K_{nr})$$

The PL lifetime τ can be expressed as the reciprocal of the sum of recombination rate constants

$$\tau = 1/(K_r+K_{nr})$$

Therefore, we can calculate the value of K_r and K_{nr} from PLQY and PL lifetime.

With the CsBr molar ratio increasing from 1.0 to 1.6, the average PL lifetime of perovskite gradually becomes shorter. The perovskite films exhibit higher non-radiative decay rates. This could be attributed to the increased surface defects caused by increased surface-area-to-volume ratio in $CsPbBr_3$ nano-domains.

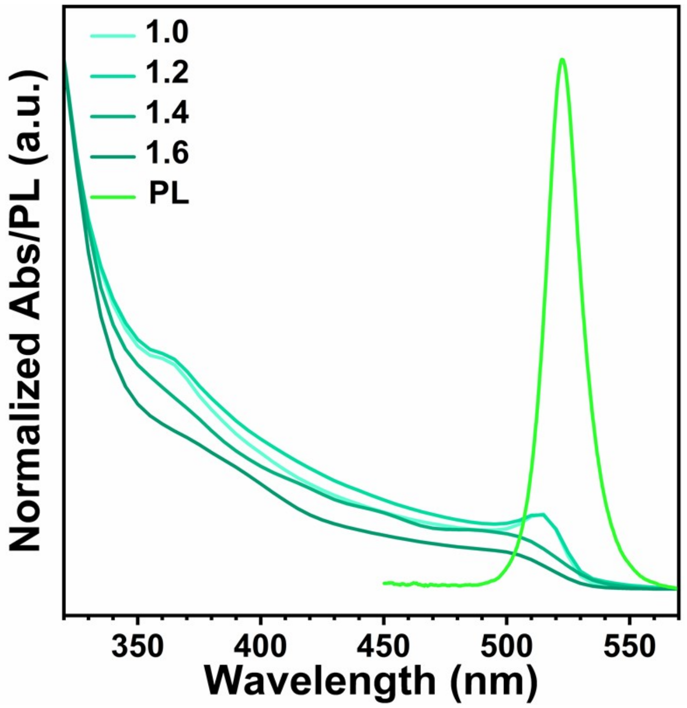

Figure S1. The normalized steady-state photoluminescence (PL) and absorption spectra of perovskite films deposited from precursor without 3-APAB (CsBr : $PbBr_2$ = x : 1, x varies from 1.0 to 1.6)

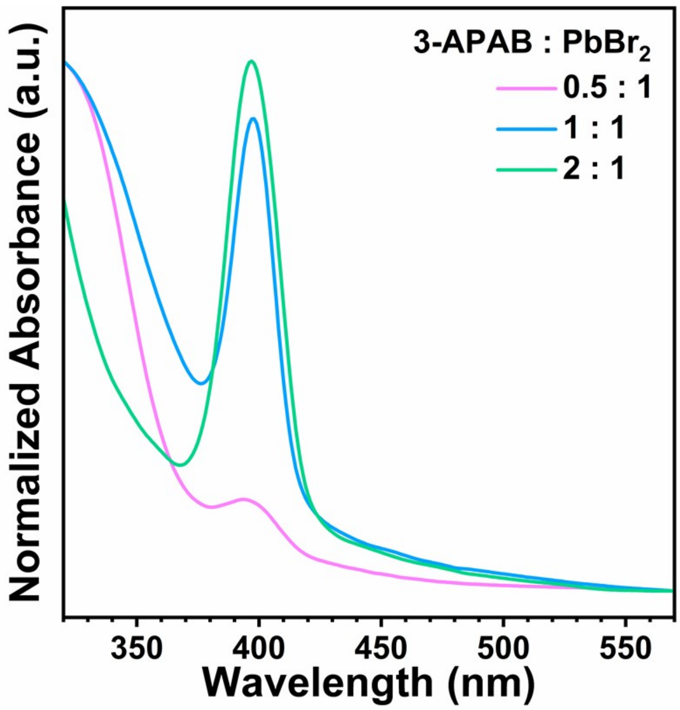

Figure S2. Absorption spectra of control films deposited with different molar ratio of 3-APAB : $PbBr_2$.

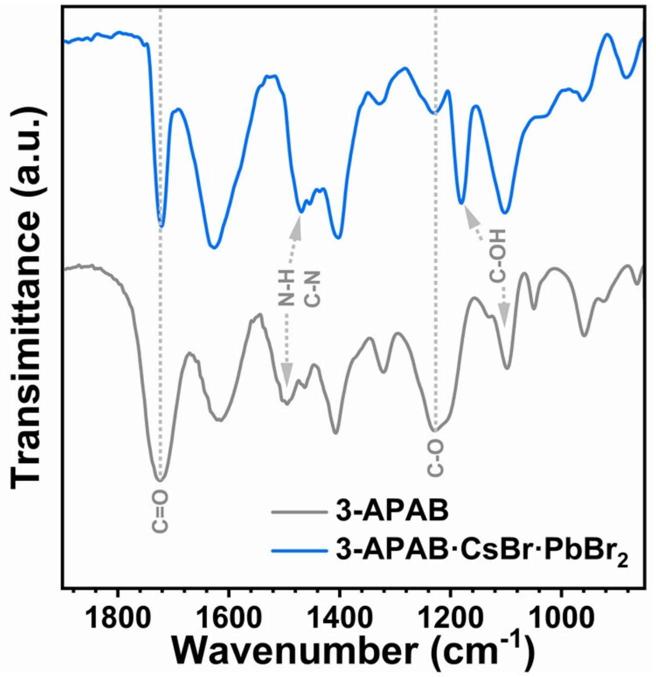

Figure S3. FTIR spectra of 3-APAB and 3-APAB with $CsPbBr_3$ perovskite. Most of the recognisable peaks from 3-APAB are still observed in the perovskite film, thus indicating that 3-APAB is present within the perovskite. The C=O and C-O stretch has weakened for the perovskite sample, which could be attributed to interactions of the carboxylate group with the perovskite crystal. The minor shifts in N-H bending vibrations could also suggest interactions of the ammonium group with the perovskite crystal.

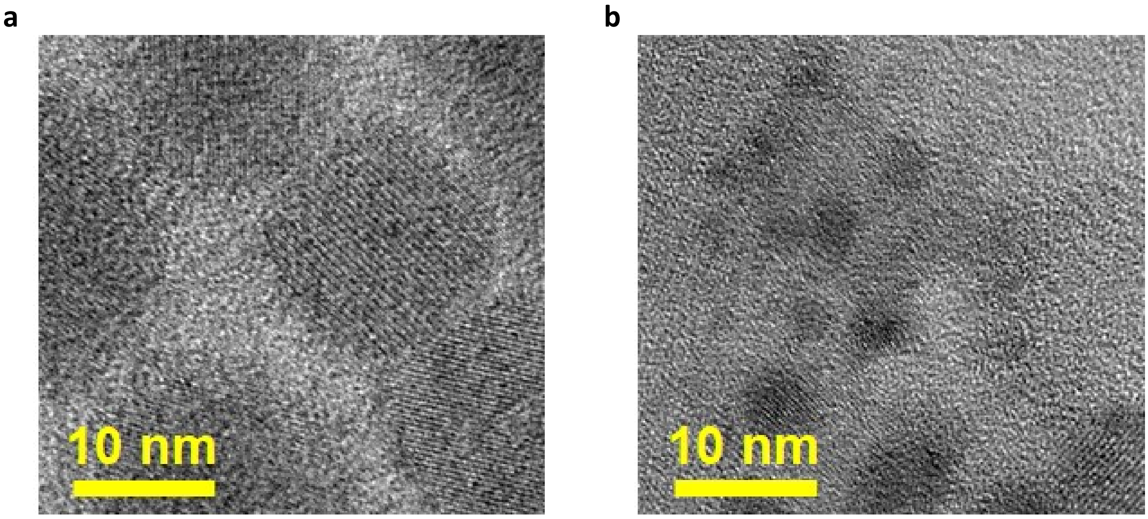

Figure S4. TEM images of $CsPbBr_3$ nano-domains formed with CsBr molar ratio of 1.0 (a) and 1.4 (b).

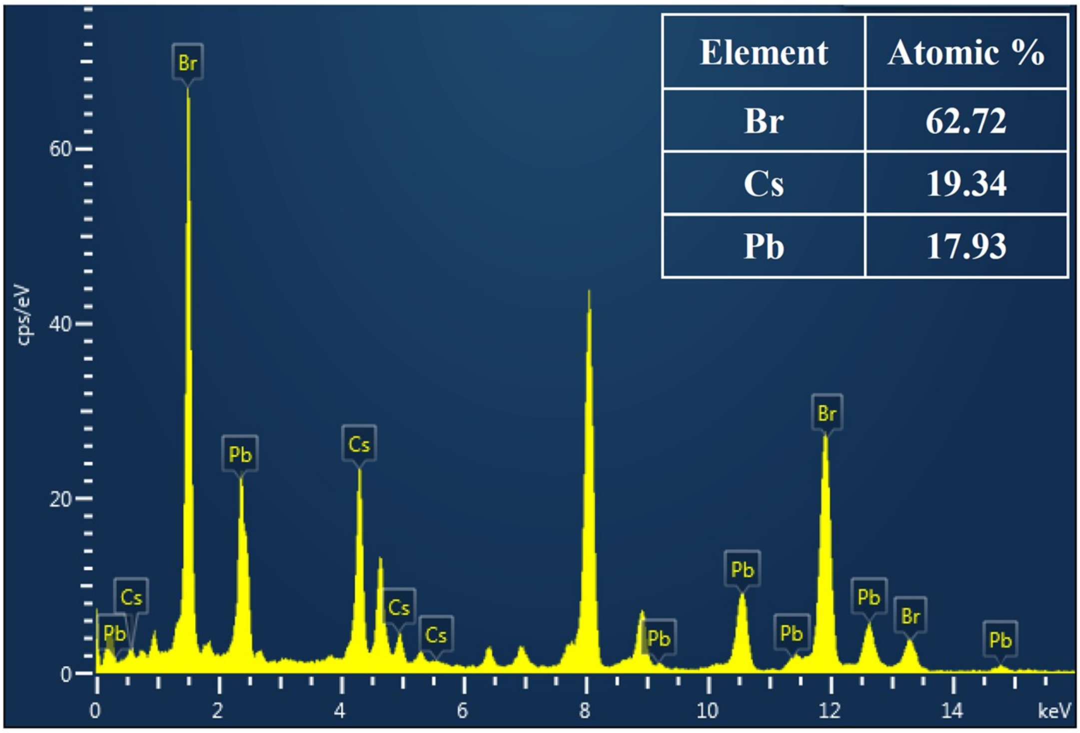

Element	Atomic %
Br	62.72
Cs	19.34
Pb	17.93

Figure S5. Energy Dispersive X-ray Spectroscopy (EDS) of the $CsPbBr_3$ films. Quantification of the EDS spectrum reveals a Cs: Pb: Br atomic ratio of 1.08 : 1 : 3.50.

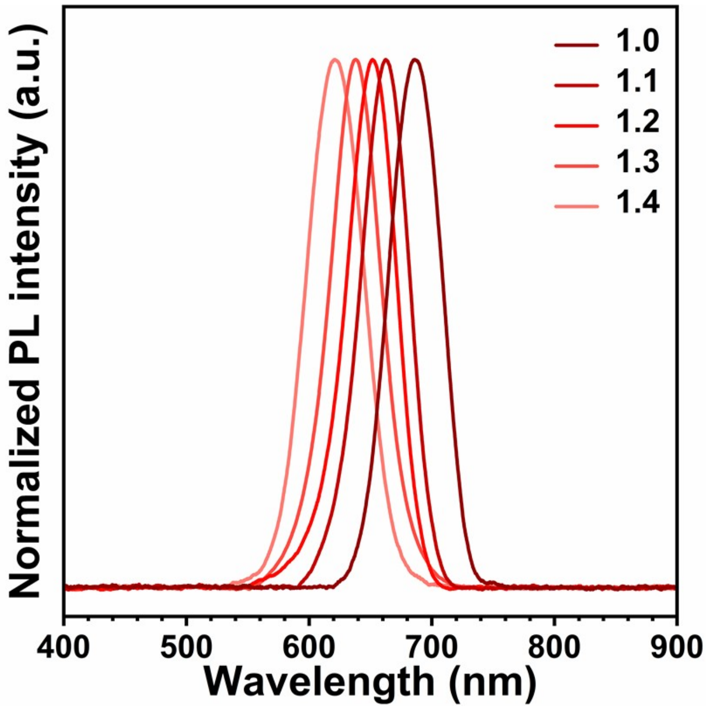

Figure S6. Normalized steady-state photoluminescence (PL) spectra with perovskite films deposited from precursor (3-APAI : CsI : PbI_2 = 1 : y : 1, y varies from 1.0 to 1.4).

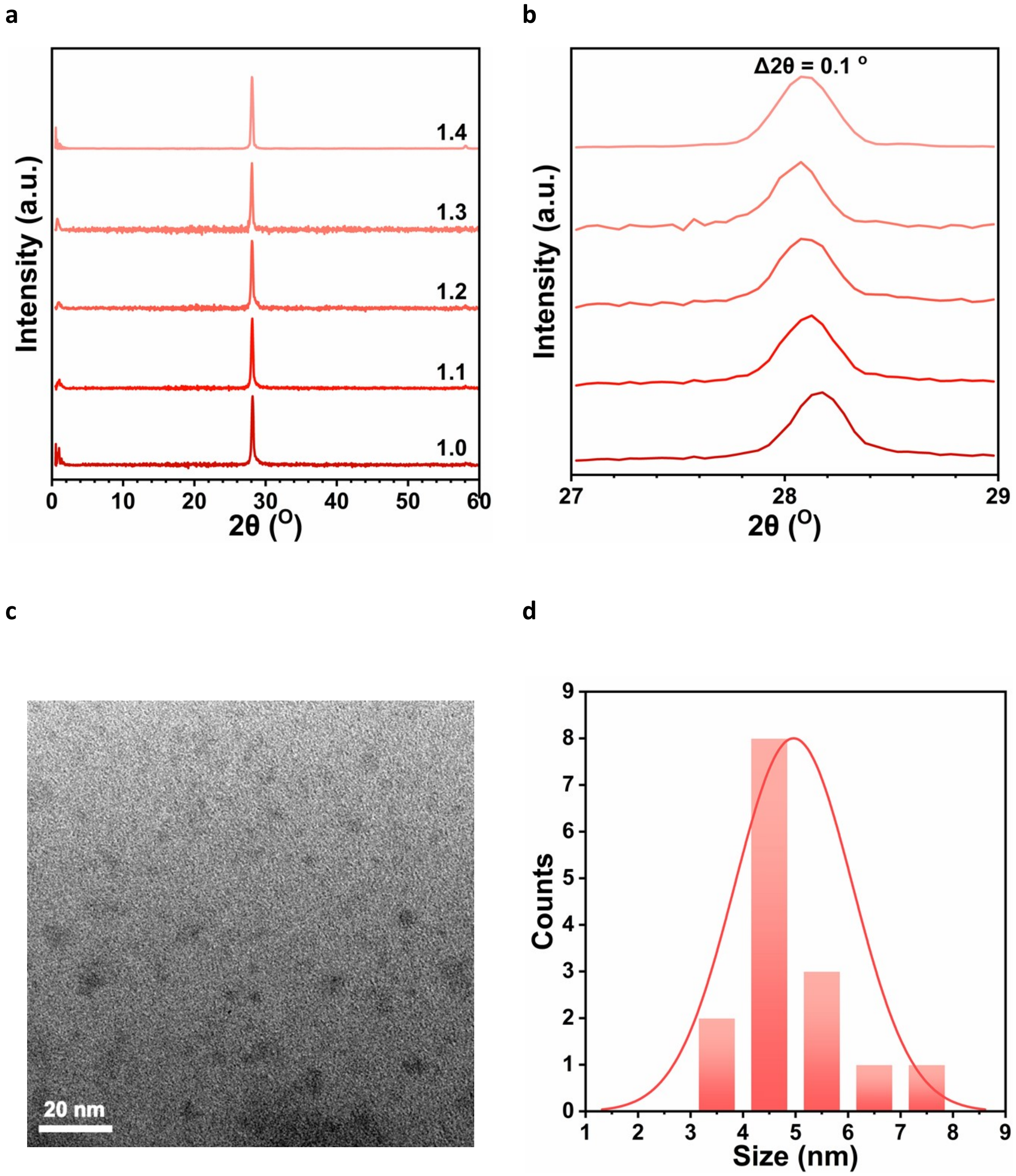

Figure S7. (a) XRD patterns of $CsPbI_3$ films deposited on silicon substrate. (b) A subtle yet monotonic shift of the (220) plane XRD peak toward a smaller diffraction degree. (c) TEM image of $CsPbI_3$ nano-domains formed with CsI (1.3) and (d) Size distribution histogram of $CsPbI_3$ nanocrystalline domains.

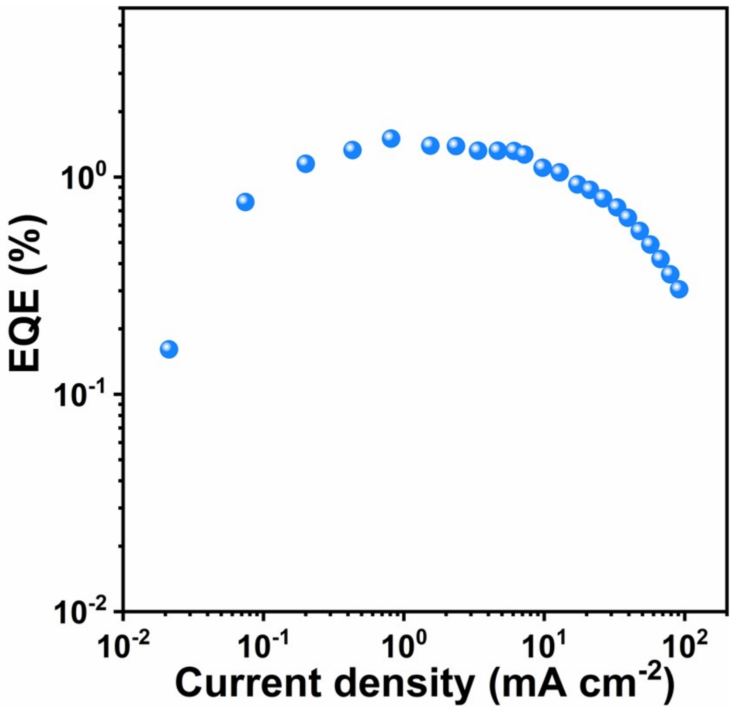

Figure S8. EQE-current density (J) curve (J-EQE) of pure-blue PeLEDs with 468 nm emission.

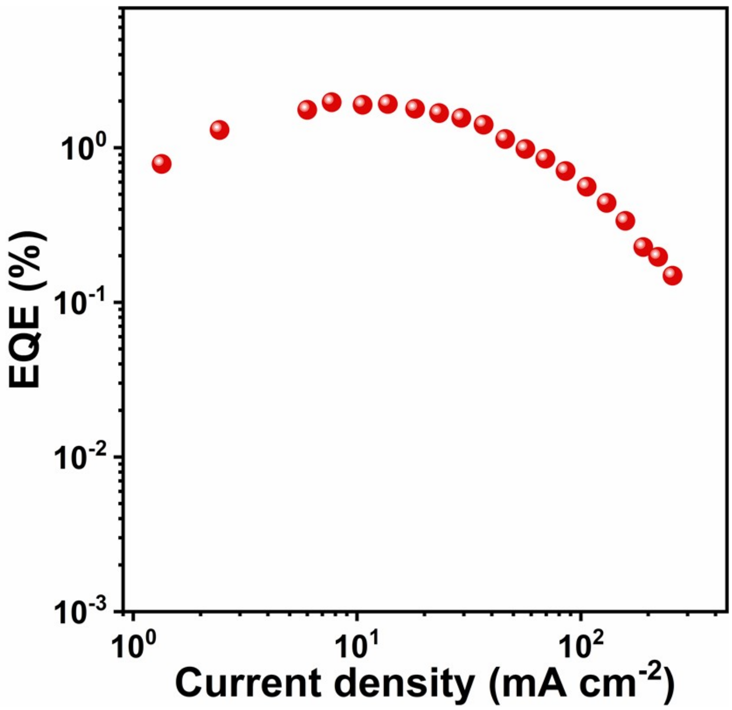

Figure S9. EQE-current density (J) curves (J-EQE) of pure-red PeLEDs with 638 nm emission.

References

1 G. Kresse, J. Furthmüller, Phys. Rev. B 1996, 54, 11169; G. Kresse, J. Furthmüller, *Comput. Mater. Sci.* **1996**, *6*, 15.

2 G. Kresse, D. Joubert, *Phys. Rev. B* **1999**, *59*, 1758.

3 J. P. Perdew, K. Burke, M. Ernzerhof, *Phys. Rev. Lett.* **1996**, *77*, 3865.

4 S. Grimme, S. Ehrlich, L. Goerigk, *J. Comput. Chem.* **2011**, *32*, 1456.

5 M. Chagas da Silva, M. Lorke, B. Aradi, M. Farzalipour Tabriz, T. Frauenheim, A. Rubio, D. Rocca, P. Deák, *Phys. Rev. Lett.* **2021**, *126*, 076401.